

Experimental status of the nuclear spin scissors mode

E.B. Balbutsev, I.V. Molodtsova

Joint Institute for Nuclear Research, 141980 Dubna, Moscow Region, Russia

P. Schuck

Institut de Physique Nucléaire, IN2P3-CNRS,

Université Paris-Sud, F-91406 Orsay Cédex, France;

*Laboratoire de Physique et Modélisation des Milieux Condensés, CNRS and Université Joseph Fourier,
25 avenue des Martyrs BP166, F-38042 Grenoble Cédex 9, France*

A new type of nuclear collective motion – the spin scissors mode – was predicted five years ago. Promising signs of its existence in ^{232}Th were found. We perform a systematic analysis of experimental data on $M1$ excitations in rare earth nuclei to find traces of the spin scissors mode in this area. Obvious signs of its existence will be demonstrated. We propose new criteria to attribute observed 1^+ states to a scissors mode, entailing that the agreement of experimental data with the results of our calculations and with the sum rule of LoIudice and Richter is improved substantially.

PACS numbers: 21.10.Hw, 21.60.Ev, 21.60.Jz, 24.30.Cz

Keywords: collective motion; scissors mode; spin; pairing

I. INTRODUCTION

In a recent paper [1] the Wigner Function Moments (WFM) or phase space moments method was applied for the first time to solve the TDHF equations including spin dynamics. As a first step, only the spin orbit interaction was included in the consideration, as the most important one among all possible spin dependent interactions because it enters into the mean field. The most remarkable result was the discovery of a new type of nuclear collective motion: rotational oscillations of "spin-up" nucleons with respect of "spin-down" nucleons (the spin scissors mode). It turns out that the experimentally observed group of peaks in the energy interval 2 – 4 MeV corresponds very likely to two different types of motion: the orbital scissors mode and this new kind of mode, i.e. the spin scissors mode. The pictorial view of these two intermingled scissors is shown in Fig. 1. It just shows the generalization of the classical picture for the orbital scissors (see, for example, [2, 3]) to include the spin scissors modes.

In Ref. [4] the influence of the spin-spin interaction on the scissors modes was studied. It was found that such interaction does not push the predicted mode strongly up in energy. It turned out that the spin-spin interaction does not change the general picture of the positions of excitations described in [1] pushing all levels up proportionally to its strength without changing their order. The most interesting result concerns the $B(M1)$ values of both scissors – the spin-spin interaction strongly redistributes $M1$ strength in favour of the spin scissors mode without changing their summed strength.

A generalization of the WFM method which takes into account spin degrees of freedom and pair correlations simultaneously was outlined in [5]. As a re-

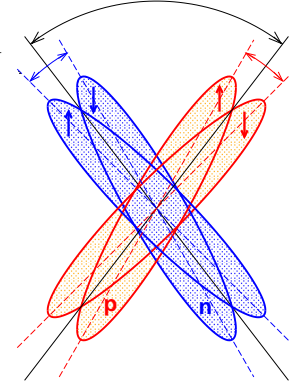


FIG. 1: Pictorial representation of two intermingled scissors: the orbital scissors (neutrons versus protons) + spin scissors (spin-up nucleons versus spin-down nucleons). Arrows inside of ellipses show the direction of spin projections. p – protons, n – neutrons.

sult the agreement between theory and experiment in the description of nuclear scissors modes was improved considerably.

The aim of the present paper is to find the experimental confirmation of our prediction: the splitting of low lying ($E < 4$ MeV) $M1$ excitations in two groups corresponding to spin and orbital scissors, the spin scissors being lower in energy and stronger in transition probability $B(M1)$. We already touched this problem in the paper [4], where we have found, that our theory explains quite naturally the experimental results of Oslo group [6] for ^{232}Th . We here will perform a systematic analysis of experimental data for rare earth nuclei, where the majority of nuclear scissors are found. It turns out that the splitting of low lying $M1$ excitations in two groups was observed and discussed by experimentalists already at the beginning of the "scissors era".

For example, we cite from the paper of C. Wesselborg in 1988 *et al.* [7]: "The existence of the two groups poses the question whether they arise from one mode, namely from scissors mode, or whether we see evidence for two independent collective modes." Prophetic words!

The paper is organized as follows. A short review of the WFM method is given in Sec. II. The experimental situation with low lying 1^+ excitations in rare earths and actinides is reviewed in Sec. III. In Sec. IV the experimental data are compared with the results of the calculations; the possibility of dividing the observed spectrum of each nucleus in two groups of levels is studied. The criteria of attributing the observed 1^+ levels to a scissors mode are analyzed in Sec. V. Exceptions from the formulated criteria are discussed in Sec. VI. The summary of main results is given in the concluding Sec. VII.

II. A FEW WORDS ABOUT WFM METHOD

The basis of our method is the Time Dependent Hartree-Fock (TDHF) equation for the one-body density matrix $\rho^\tau(\mathbf{r}_1, \mathbf{r}_2, t) = \langle \mathbf{r}_1 | \hat{\rho}^\tau(t) | \mathbf{r}_2 \rangle$:

$$i\hbar \frac{\partial \hat{\rho}^\tau}{\partial t} = [\hat{h}^\tau, \hat{\rho}^\tau], \quad (1)$$

where τ is an isotopic index. It is convenient to modify equation (1) introducing the Wigner transform [8] of the density matrix

$$f^\tau(\mathbf{r}, \mathbf{p}, t) = \int d\mathbf{s} \exp(-i\mathbf{p} \cdot \mathbf{s}/\hbar) \rho^\tau\left(\mathbf{r} + \frac{\mathbf{s}}{2}, \mathbf{r} - \frac{\mathbf{s}}{2}, t\right) \quad (2)$$

and of the Hamiltonian

$$h_W^\tau(\mathbf{r}, \mathbf{p}) = \int d\mathbf{s} \exp(-i\mathbf{p} \cdot \mathbf{s}/\hbar) \left(\mathbf{r} + \frac{\mathbf{s}}{2} \left| \hat{h}^\tau \right| \mathbf{r} - \frac{\mathbf{s}}{2} \right). \quad (3)$$

Performing the Wigner transformation of (1) one derives the dynamical equation for the Wigner function $f^\tau(\mathbf{r}, \mathbf{p}, t)$ [9]:

$$\frac{\partial f^\tau}{\partial t} = \frac{2}{\hbar} \sin \left\{ \frac{\hbar}{2} \sum_{\alpha=-1}^1 (-1)^\alpha \cdot [(\nabla_{-\alpha})^h \cdot (\nabla_\alpha^p)^f - (\nabla_{-\alpha}^p)^h \cdot (\nabla_\alpha)^f] \right\} h_W^\tau f^\tau. \quad (4)$$

Here the upper index on the bracket stands for the function on which the operator in these brackets

acts. The equation is written in terms of cyclic variables

$$r_{\pm 1} = \mp \frac{1}{\sqrt{2}}(x_1 \pm ix_2), \quad r_0 = x_3, \\ \nabla_{\pm 1} = \mp \frac{1}{\sqrt{2}}\left(\frac{\partial}{\partial x_1} \pm i \frac{\partial}{\partial x_2}\right), \quad \nabla_0 = \frac{\partial}{\partial x_3}, \quad (5)$$

that allows one to use the technique of tensor products [10] in the following.

Let us consider the simple Hamiltonian:

$$H = \sum_{i=1}^A \left(\frac{\mathbf{p}_i^2}{2m} + \frac{1}{2} m \omega^2 \mathbf{r}_i^2 \right) \\ + \sum_{\mu=-2}^2 (-1)^\mu \left\{ \bar{\kappa} \sum_i^Z \sum_j^N \right. \\ \left. + \frac{\kappa}{2} \left[\sum_{i \neq j}^Z + \sum_{i \neq j}^N \right] \right\} q_{2\mu}(\mathbf{r}_i) q_{2-\mu}(\mathbf{r}_j), \quad (6)$$

where $q_{2\mu} = \sqrt{16\pi/5} r^2 Y_{2\mu}$ and N, Z are the numbers of neutrons and protons respectively. The mean field potential for nucleons is

$$V^\tau(\mathbf{r}, t) = \frac{m}{2} \omega^2 r^2 + 6 \sum_{\mu=-2}^2 (-1)^\mu Z_{2-\mu}^\tau(t) \{r \otimes r\}_{2\mu}, \quad (7)$$

where $Z_{2\mu}^n = \kappa R_{2\mu}^n + \bar{\kappa} R_{2\mu}^p$, $Z_{2\mu}^p = \kappa R_{2\mu}^p + \bar{\kappa} R_{2\mu}^n$ and the quadrupole moments $R_{2\mu}^\tau(t)$ are defined in Eq. (9) below.

Integrating the equation (4) over phase space with the weights

$$W = \{r \otimes p\}_{\lambda\mu}, \{r \otimes r\}_{\lambda\mu}, \{p \otimes p\}_{\lambda\mu}, \quad (8)$$

where $\{r \otimes p\}_{\lambda\mu} = \sum_{\sigma, \nu} C_{1\sigma, 1\nu}^{\lambda\mu} r_\sigma p_\nu$ and $C_{1\sigma, 1\nu}^{\lambda\mu}$ is the Clebsch-Gordan coefficient, one gets dynamic equations for second order moments

$$R_{\lambda\mu}^\tau(t) = \frac{2}{(2\pi\hbar)^3} \int d\mathbf{p} \int d\mathbf{r} \{r \otimes r\}_{\lambda\mu} f^\tau(\mathbf{r}, \mathbf{p}, t), \\ P_{\lambda\mu}^\tau(t) = \frac{2}{(2\pi\hbar)^3} \int d\mathbf{p} \int d\mathbf{r} \{p \otimes p\}_{\lambda\mu} f^\tau(\mathbf{r}, \mathbf{p}, t), \\ L_{\lambda\mu}^\tau(t) = \frac{2}{(2\pi\hbar)^3} \int d\mathbf{p} \int d\mathbf{r} \{r \otimes p\}_{\lambda\mu} f^\tau(\mathbf{r}, \mathbf{p}, t), \quad (9)$$

which play the role of the collective variables.

Dynamic equations are:

$$\begin{aligned}
\frac{d}{dt}R_{\lambda\mu}^\tau - \frac{2}{m}L_{\lambda\mu}^\tau &= 0, & \lambda = 0, 2 \\
\frac{d}{dt}L_{\lambda\mu}^\tau - \frac{1}{m}P_{\lambda\mu}^\tau + m\omega^2 R_{\lambda\mu}^\tau - 12\sqrt{5}\sum_{j=0}^2\sqrt{2j+1}\{\begin{smallmatrix} 11j \\ 2\lambda 1 \end{smallmatrix}\}\{Z_2^\tau \otimes R_j^\tau\}_{\lambda\mu} &= 0, & \lambda = 0, 1, 2 \\
\frac{d}{dt}P_{\lambda\mu}^\tau + 2m\omega^2 L_{\lambda\mu}^\tau - 24\sqrt{5}\sum_{j=0}^2\sqrt{2j+1}\{\begin{smallmatrix} 11j \\ 2\lambda 1 \end{smallmatrix}\}\{Z_2^\tau \otimes L_j^\tau\}_{\lambda\mu} &= 0, & \lambda = 0, 2
\end{aligned} \tag{10}$$

where $\{\begin{smallmatrix} 11j \\ 2\lambda 1 \end{smallmatrix}\}$ is the Wigner $6j$ -symbol.

Equations (10) are exact, because they are derived from (1) without any approximations. They are nonlinear and must be solved numerically for arbitrary amplitudes. In this way, the effects of anharmonicity in multiphonon giant monopole and quadrupole resonances were studied in [11]. In a small amplitude approximation, after approximate separation of equations for isoscalar and isovector variables, the system (10) becomes analytically solvable. Both, isovector and isoscalar equations were studied in [9, 12]. The analytic expressions for energies, transition probabilities and lines of currents were found. The analysis of dynamical equations and their solutions allowed us to demonstrate in an obvious way three essential properties of the scissors mode:

1. its inevitable coupling with IsoVector Giant Quadrupole Resonance (IVGQR),
2. the energy of this kind of motion differs from zero only due to Fermi surface deformation,
3. lines of current for scissors mode are ellipses (rotational motion) and that of IVGQR are hyperbolae (irrotational motion) (see Fig. 2).

The last finding is especially important, because it proves that the popular interpretation of the 1^+ branch of IVGQR as a giant scissors mode is erroneous. Such misunderstanding is easily explainable, because this excitation has a $B(M1)$ value of the same order of magnitude, as the scissors mode. However, the expected rotational motion is suppressed by the irrotational one which manifests itself by the huge $B(E2)$ value.

In spite of the evident success of equations (10) in the description of all qualitative features of the scissors mode, their ability in reproducing its quantitative characteristics turned out rather poor (see Fig. 3) – the calculated $B(M1)$ values exceed the experimental ones 3 – 5 times, whereas the calculated energies are 2 – 5 times smaller than experimental values. However, further developments of the WFM method [13, 14], namely, the switch from

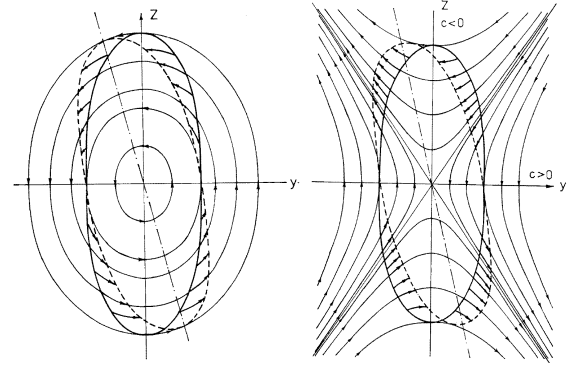


FIG. 2: Schematic picture of isovector displacements for the scissors mode (left) and IVGQR (right). The lines of currents are shown by thin lines: ellipses for scissors mode and hyperbolae for IVGQR. The thick oval is the initial position of the nucleus' surface (common for protons and neutrons). The dashed oval is the final position of the protons' (or neutrons') surface as a result of infinitesimal displacements shown by the arrows.

TDHF to TDHFB equations to include the pair correlations, improved the situation considerably (see Fig. 3). Now the theoretical $B(M1)$ values exceed the experimental ones only 2 – 3 times and the theoretical energies exceed the experimental ones only by a factor of 1.1 – 1.2. The improvement is of course impressive, but not satisfactory, especially for transition probabilities. It becomes satisfactory (see Fig. 3) after the generalization of the WFM method to take into account pair correlations and spin degrees of freedom simultaneously [5].

The decisive role in the substantial improvement of results is played by the anti-aligned spins [5]. These momenta generate a new type of nuclear collective motion – rotational oscillations of "spin-up" nucleons with respect of "spin-down" nucleons. We called this motion 'spin scissors mode'. It is disposed (in energy) below the conventional (orbital) scissors mode and exceeds the one in the magnetic strength. A typical example of calculated energies and $B(M1)$ values of both scissors modes is given in Table I.

TABLE I: Scissors modes energies E and transition probabilities $B(M1)$ for ^{164}Dy .

	E (MeV)			$B(M1)$ (μ_N^2)		Σ
	spin scissors	orbital scissors	centroid	spin scissors	orbital scissors	
$g_s \neq 0$	2.77	3.60	3.07	2.44	1.36	3.80
$g_s = 0$	2.77	3.60	3.50	0.76	6.10	6.86

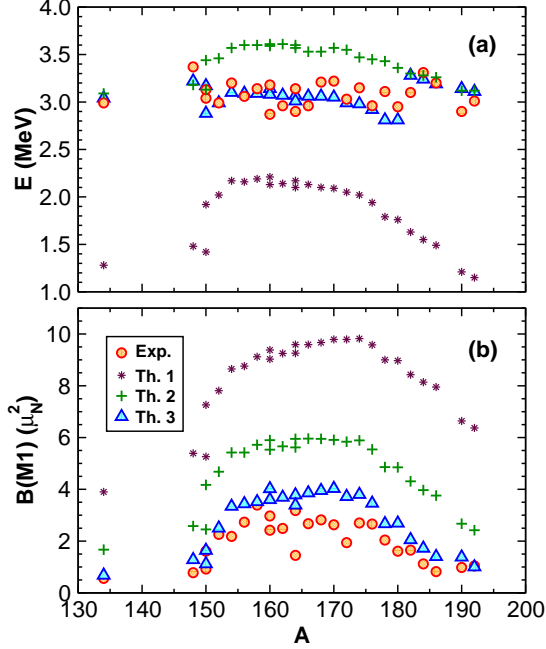


FIG. 3: The energies E (a) and $B(M1)$ -factors (b) as a function of the mass number A . The experimental values of E and $B(M1)$ are from [15, 16] and references therein. Th. 1 – the results of calculations without spin degrees of freedom and pair correlations, Th. 2 – pairing is included, Th. 3 – pairing and spin degrees of freedom are taken into account.

The results of the calculations with and without the spin part of a dipole magnetic operator

$$\hat{O}_{11} = \frac{\mu_N}{\hbar} \sqrt{\frac{3}{4\pi}} \left[g_s \hat{S}_1 + g_l \hat{l}_1 \right], \quad (11)$$

($g_s \neq 0$ and $g_s = 0$ respectively) show that both scissors are equally sensitive to the spin dependent part of nuclear forces, demonstrating the moderate constructive interference of the orbital and spin contributions in the case of the spin scissors mode and their very strong destructive interference in the case of the orbital scissors mode.

III. EXPERIMENTAL SITUATION

The natural question arises: is it possible to observe the spin scissors mode experimentally?

A. Rare earths

We have studied practically all papers with experimental data for low lying $M1$ excitations in rare earth nuclei. For the sake of convenience we have collected in Fig. 4 all experimentally known spectra of low lying 1^+ excitations [17–31]. It should be emphasized, that only the levels with positive parities are displayed here. As a matter of fact, there exist many 1^π excitations in the energy interval 1 – 4 MeV, whose parities π are not known up to now.

One glance on Fig. 4 is enough to understand that the situation with spectra in rare earth nuclei is very complicated. We have in mind the possible concentration of the observed 1^+ excitations in two more or less separated groups. It is seen, that spectra of only 8 nuclei (out of 32 ones) can be divided in two groups with certainty: ^{146}Nd , ^{154}Gd , $^{160,162}\text{Dy}$, ^{170}Er , ^{176}Yb , ^{178}Hf and ^{190}Os . Of course, experimentalists paid heed to, and discussed, this feature of the mentioned spectra – see, for example, the citation from [7] in the Introduction. The division of other spectra in two groups is not so obvious. To facilitate this task we allotted all lines of spectra by the artificial widths and joined them by Lorentzian's curves. The value of width was chosen big enough to reduce the number of humps to a minimum. The result is shown on Fig. 4. It is easy to see that the spectra of 13 additional nuclei can be represented by two-humps curves. One can divide each of those spectra in two groups taking the point of minimum between two humps as the border between two groups of levels. These nuclei are ^{150}Nd , ^{150}Sm , $^{156,160}\text{Gd}$, ^{164}Dy , ^{168}Er , $^{176,180}\text{Hf}$, $^{182,184,186}\text{W}$, ^{192}Os and ^{194}Pt . There are also 9 nuclei, where we see three or more humps: ^{134}Ba , $^{144,148}\text{Nd}$, ^{154}Sm , ^{158}Gd , ^{166}Er , $^{172,174}\text{Yb}$ and ^{196}Pt . Here one must choose, which minimum to take as the border. Naturally, our choice was guided by the results of our calculations, which predict, as a rule, that the lower in energy scissors (spin scissors) is stronger than the higher one (orbital scissors). This means that the minimum on the right hand side (r.h.s.) will be chosen – the only exception is ^{144}Nd , where the minimum on the left is chosen because $B(M1)_{\text{sp}} < B(M1)_{\text{or}}$ in theory.

And finally, there are two nuclei with a single hump, because they have only one compact group

of levels: $^{148,152}\text{Sm}$. Naturally, the separation here is impossible.

B. Actinides

The experimental spectra of 1^+ excitations of three actinide nuclei [32–34] are shown on Fig. 5. Only the spectrum of ^{232}Th can be divided in two groups with certainty. The spectra of both uranium nuclei can be divided only with the help of Lorentzians.

IV. COMPARISONS

The values of $B(M1)$ and energies, corresponding to the described rules of separation, are compared with theoretical results in the Tables II, III and on Fig. 6. The details of WFM calculations can be found in [5].

A. Splitting in rare earths

Let us analyze Table II and Fig. 6.

Here the data on 32 nuclei are collected. According to the theoretical data the spin scissors mode is stronger than the orbital scissors in 29 nuclei and only in three weakly deformed nuclei ($^{144,146}\text{Nd}$ and ^{148}Sm) the situation is opposite. The qualitative agreement between experimental data and theory is observed in 15 nuclei: ^{134}Ba , $^{146,148,150}\text{Nd}$, $^{150,154}\text{Sm}$, ^{154}Gd , ^{160}Dy , $^{172,174,176}\text{Yb}$, $^{176,180}\text{Hf}$ and $^{190,192}\text{Os}$ – the spin scissors is stronger or weaker (in ^{146}Nd) than orbital one. It is difficult to estimate objectively the degree of quantitative agreement, so we will try to give our subjective appraisal. Looking attentively on Fig. 6 and Table II one can find the satisfactory (mostly very good) agreement between theoretical and experimental results for the orbital scissors ($B(M1)$ and energies) in 19 nuclei: ^{134}Ba , $^{144,146,148,150}\text{Nd}$, ^{150}Sm , ^{154}Gd , $^{166,170}\text{Er}$, $^{174,176}\text{Yb}$, $^{176,178,180}\text{Hf}$, ^{184}W , $^{190,192}\text{Os}$ and $^{194,196}\text{Pt}$. The same degree of agreement can be found for the spin scissors in 16 nuclei: ^{134}Ba , $^{148,150}\text{Nd}$, $^{150,154}\text{Sm}$, ^{154}Gd , ^{160}Dy , $^{172,174,176}\text{Yb}$, $^{176,180}\text{Hf}$, $^{190,192}\text{Os}$ and $^{194,196}\text{Pt}$. Therefore the satisfactory (frequently very good) agreement between theoretical and experimental results for both, the orbital and spin scissors, is observed in 13 nuclei: ^{134}Ba , $^{148,150}\text{Nd}$, ^{150}Sm , ^{154}Gd , $^{174,176}\text{Yb}$, $^{176,180}\text{Hf}$, $^{190,192}\text{Os}$ and $^{194,196}\text{Pt}$. 40 % – not so bad!

What about the remaining 19 nuclei? We know (see Sec. IV C and Fig. 7) that sums of experimental $B(M1)$ values and the respective energy centroids agree (with rare exceptions) very well with

theoretical ones. This means that, if not to take into account the natural division of levels in separate groups, one can always divide the experimental spectrum of any nucleus into two such groups that the summed $B(M1)$ value and respective energy of each group will be in perfect agreement with theoretical one. Of course, it will be pure fitting which will not satisfy anybody, because it does not help to understand the genuine reason of levels grouping. So, one can do the following inference: the WFM method gives the satisfactory (with minor exceptions) description of global properties of the scissors mode and does not describe (in 60% of cases) its fine structure. However, this statement is only half true. It is necessary to remember that we take into account only second order moments. As a consequence our input information about nuclei is very restricted – it is the number of protons Z and neutrons N , the monopole moment Q_{00} (mean square radius), the quadrupole moment Q_{20} (deformation) and the equilibrium angular momentum of nucleons with spin projection up (or down) L_{10} . Naturally, it is difficult to expect, that the knowledge of so small number of internal characteristics of nucleus will be sufficient to describe the fine structure of its excitations. A more detailed input is required! The natural origin of the additional information in the method of moments is obvious – that are higher order moments. We are sure that the inclusion of the fourth order moments will allow us to improve substantially the description of the scissors mode fine structure. It is the task for future publications.

B. Splitting in actinides

Let us analyze Table III.

It is seen, that there is rather good agreement between the theory and experiment for both scissors in ^{232}Th ; the agreement in ^{236}U can be characterized as "not so bad". There is not even a qualitative agreement in ^{238}U – nevertheless one can hope that situation here can be improved substantially (see Sec. VI).

C. Summarized values

The summarized $B(M1)$ values together with the respective energy centroids are collected in Table IV; they are demonstrated also in Fig. 7.

Thus, let us study Fig. 7. Here the results of the calculations with the WFM method are compared with four variants of experimental data treatments. The Fig. 7(a,a') is just a part of Fig. 3. Here the results of our calculations (sums of spin and orbital scissors strengths and the respective energy centroids) are compared with experimental data from

TABLE II: Energy centroids E and summed transition probabilities $B(M1)$ of the spin scissors and the orbital scissors; spectra are taken from papers shown in the last column of Table IV. The information for many nuclei contains second line, which is obtained by taking into account 1^+ states together with 1^π states with π unknown.

Nuclei	E (MeV)						$B(M1)$ (μ_N^2)					
	spin scissors		orbital scissors		centroid		spin scissors		orbital scissors		Σ	
	Exp.	WFM	Exp.	WFM	Exp.	WFM	Exp.	WFM	Exp.	WFM	Exp.	WFM
^{134}Ba	2.88	3.02	3.35	3.43	2.99	3.04	0.43(06)	0.65	0.13(03)	0.03	0.56(09)	0.68
	2.85		3.65		3.33		0.51(08)		0.76(16)		1.26(24)	
^{144}Nd	2.57	2.97	3.57	3.32	3.07	3.21	0.39(03)	0.06	0.39(02)	0.14	0.78(05)	0.20
	2.63		3.64		3.22		0.51(05)		0.70(06)		1.21(11)	
^{146}Nd	2.36	3.00	3.37	3.38	2.90	3.20	0.34(04)	0.27	0.39(06)	0.30	0.73(10)	0.57
	2.38		3.60		3.28		0.38(05)		1.08(18)		1.45(23)	
^{148}Nd	3.22	3.09	3.83	3.54	3.40	3.22	0.80(19)	0.91	0.32(07)	0.37	1.12(26)	1.28
^{150}Nd	3.02	2.90	3.72	3.64	3.12	3.13	1.56(21)	1.27	0.27(05)	0.56	1.83(26)	1.83
^{148}Sm	—	2.98	—	3.35	3.07	3.17	—	0.22	—	0.24	0.51(12)	0.46
^{150}Sm	3.07	3.06	3.73	3.49	3.18	3.17	0.81(12)	0.84	0.16(05)	0.27	0.97(17)	1.12
^{152}Sm	—	2.71	—	3.53	2.97	2.99	—	1.65	—	0.85	2.41(33)	2.50
^{154}Sm	2.98	2.79	3.62	3.64	3.14	3.10	2.08(30)	2.12	0.68(20)	1.22	2.76(50)	3.34
^{154}Gd	2.91	2.75	3.10	3.58	3.00	3.04	1.40(25)	1.95	1.20(25)	1.05	2.60(50)	3.00
^{156}Gd	2.28	2.79	3.06	3.63	2.94	3.09	0.49(12)	2.19	2.73(56)	1.24	3.22(68)	3.44
^{158}Gd	2.64	2.78	3.20	3.62	3.04	3.09	1.13(23)	2.25	2.86(42)	1.27	3.99(65)	3.52
^{160}Gd	2.65	2.82	3.33	3.67	3.10	3.14	1.53(14)	2.53	2.88(40)	1.49	4.41(54)	4.02
^{160}Dy	2.84	2.78	3.06	3.61	2.87	3.08	2.12(25)	2.30	0.30(05)	1.30	2.42(30)	3.60
^{162}Dy	2.44	2.78	2.96	3.60	2.84	3.07	0.71(05)	2.37	2.59(19)	1.32	3.30(24)	3.69
^{164}Dy	2.60	2.77	3.17	3.60	3.00	3.07	1.67(14)	2.44	3.85(31)	1.36	5.53(45)	3.80
^{166}Er	2.36	2.77	3.21	3.59	2.79	3.06	1.52(34)	2.48	1.60(24)	1.38	3.12(58)	3.86
	2.37		3.25		2.85		1.56(35)		1.86(46)		3.42(81)	
^{168}Er	2.72	2.77	3.43	3.58	3.21	3.06	1.21(14)	2.54	2.63(35)	1.41	3.85(50)	3.95
	2.69		3.46		3.22		1.35(17)		3.04(44)		4.38(61)	
^{170}Er	2.79	2.76	3.39	3.57	3.22	3.05	0.75(11)	2.60	1.88(28)	1.43	2.63(39)	4.03
	2.77		3.42		3.21		1.07(19)		2.24(41)		3.30(59)	
^{172}Yb	2.75	2.72	3.60	3.51	2.93	2.99	1.88(37)	2.46	0.49(12)	1.26	2.37(49)	3.72
	2.77		3.73		3.07		1.99(41)		0.94(26)		2.93(67)	
^{174}Yb	2.56	2.72	3.49	3.50	2.96	2.98	1.89(70)	2.51	1.44(51)	1.29	3.33(1.21)	3.80
	2.35		3.29		2.97		1.19(52)		2.28(76)		3.47(1.28)	
^{176}Yb	2.52	2.68	3.73	3.44	2.86	2.92	2.32(60)	2.34	0.92(45)	1.12	3.24(1.05)	3.46
	2.52		3.65		2.98		2.32(60)		1.60(70)		3.92(1.30)	
^{176}Hf	2.89	3.06	3.70	3.73	3.22	3.27	1.99(15)	2.15	1.33(13)	1.00	3.32(28)	3.15
	2.91		3.69		3.25		2.47(22)		1.93(23)		4.40(45)	
^{178}Hf	2.79	3.05	3.64	3.72	3.21	3.27	1.19(11)	2.18	1.19(22)	1.02	2.38(33)	3.20
	2.73		3.67		3.15		1.19(11)		1.38(26)		2.57(37)	
^{180}Hf	2.84	3.02	3.75	3.67	3.16	3.22	1.38(17)	1.97	0.75(13)	0.86	2.13(30)	2.84
	2.84		3.80		3.30		1.57(22)		1.43(27)		3.00(49)	
^{182}W	2.47	2.96	3.25	3.57	3.10	3.13	0.31(05)	1.48	1.34(23)	0.55	1.65(28)	2.03
^{184}W	2.58	2.94	3.62	3.52	3.19	3.08	0.51(10)	1.27	0.73(27)	0.41	1.24(37)	1.68
^{186}W	2.56	2.91	3.29	3.48	3.19	3.03	0.11(01)	1.06	0.71(20)	0.29	0.82(21)	1.36
	2.56		3.36		3.29		0.11(01)		1.18(64)		1.29(65)	
^{190}Os	2.64	2.87	3.11	3.25	2.83	2.98	0.56(08)	1.01	0.38(04)	0.38	0.94(12)	1.39
	2.14		3.37		2.72		1.26(19)		1.12(16)		2.38(36)	
^{192}Os	2.95	2.85	3.34	3.21	3.00	2.94	0.79(04)	0.74	0.14(02)	0.25	0.93(06)	0.99
	2.89		3.40		3.07		1.16(08)		0.63(06)		1.78(14)	
^{194}Pt	2.92	2.82	3.52	3.16	3.25	2.97	0.57(09)	0.66	0.74(14)	0.52	1.31(23)	1.17
	2.92		3.51		3.29		0.57(09)		0.93(17)		1.50(25)	
^{196}Pt	2.50	2.81	2.82	3.12	2.70	2.95	0.27(05)	0.46	0.42(07)	0.40	0.69(13)	0.86
	2.50		2.93		2.79		0.27(05)		0.55(15)		0.82(20)	

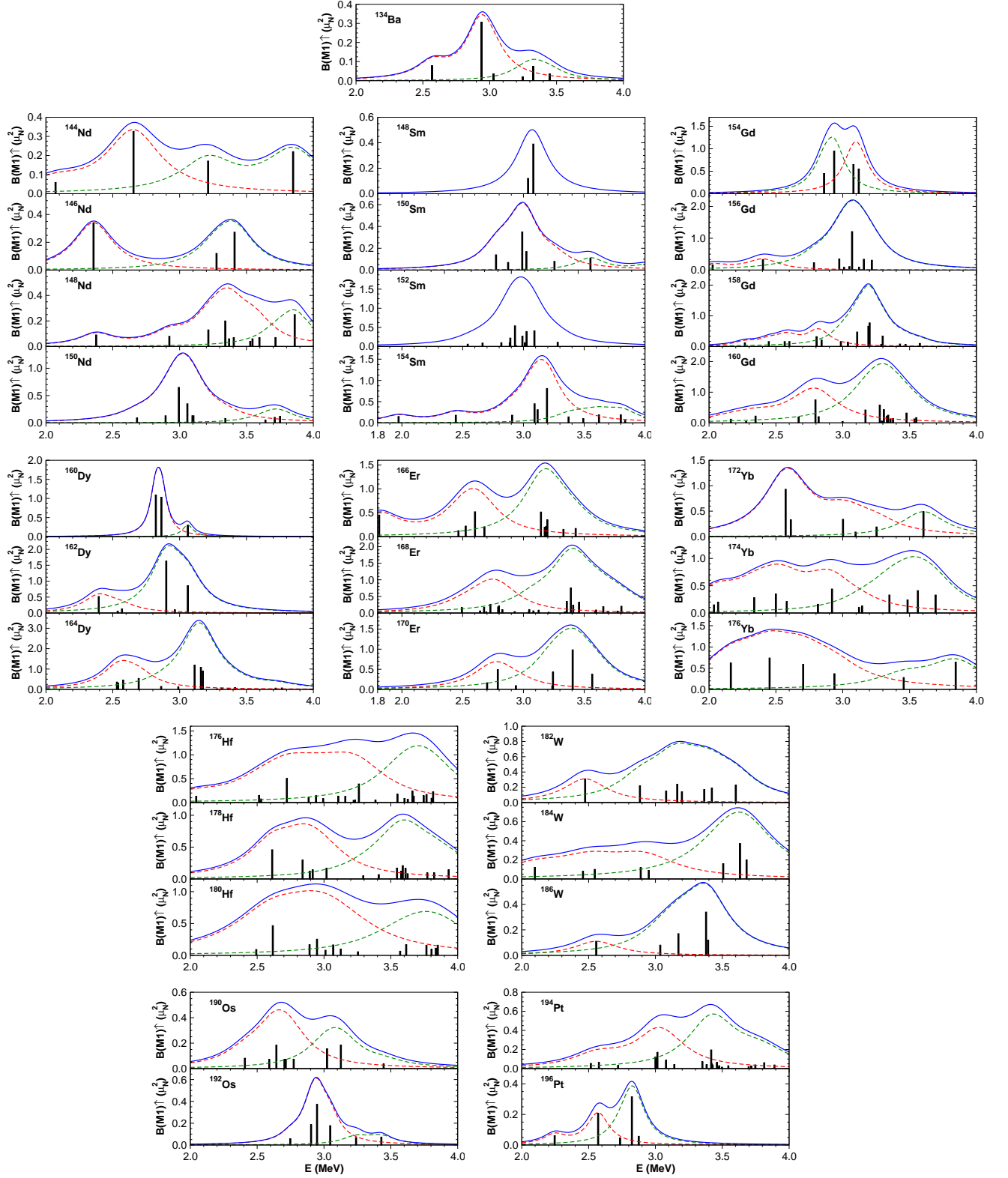


FIG. 4: The experimentally observed spectra of 1^+ excitations: ^{134}Ba – [17], $^{144-150}\text{Nd}$ – [18, 19], $^{148-154}\text{Sm}$ – [20], $^{154-160}\text{Gd}$ – [21, 22], $^{160-164}\text{Dy}$ – [7, 23], $^{166-170}\text{Er}$ – [24], $^{172-176}\text{Yb}$ – [25], $^{176-180}\text{Hf}$ – [26, 27], $^{182-186}\text{W}$ – [28], $^{190-192}\text{Os}$ – [29], $^{194-196}\text{Pt}$ – [30, 31]. The lines of spectra are allotted by artificial widths and joined by Lorentzian's curves (thick curves for all lines, dashed curves for two separate groups attributed to spin and orbital scissors).

TABLE III: The same as in Table II but for actinide nuclei.

Nuclei	E (MeV)						$B(M1)$ (μ_N^2)					
	spin scissors		orbital scissors		centroid		spin scissors		orbital scissors		Σ	
	Exp.	WFM	Exp.	WFM	Exp.	WFM	Exp.	WFM	Exp.	WFM	Exp.	WFM
^{232}Th	2.15	2.30	2.99	2.93	2.49(37)	2.54	2.52(26)	2.40	1.74(38)	1.42	4.26(64)	3.82
^{236}U	2.10	2.33	2.61	2.96	2.33	2.57	2.01(25)	2.83	1.60(26)	1.73	3.61(51)	4.56
	2.12		2.63		2.35		2.26(29)		1.80(31)		4.06(60)	
^{238}U	2.19	2.36	2.76	3.00	2.58	2.61	2.46(31)	3.18	5.13(89)	2.02	7.59(1.20)	5.20

TABLE IV: Mean excitation energies and summed $M1$ strengths of the scissors mode corresponding to different treatment of experimental data (see Sec. V): Ref. [15], Ref. [16], Ref. [35] – review papers, Exp. – our treatment of experimental data taken from original papers shown in the last column, WFM – theory.

Nuclei	δ	E (MeV)				$B(M1)$ (μ_N^2)				Ref.
		Ref. [16]	Ref. [35]	Exp.	WFM	Ref. [15]	Ref. [35]	Exp.	WFM	
^{134}Ba	0.14	2.99	2.99	2.99	3.04	–	0.56(09)	0.56(09)	0.68	[17]
^{144}Nd	0.12	3.21	3.15	3.07	3.21	–	0.72(05)	0.78(05)	0.20	[18]
^{146}Nd	0.13	3.47	3.46	2.90	3.20	0.72(06)	0.94(17)	0.73(10)	0.57	[19]
^{148}Nd	0.17	3.37	3.49	3.40	3.22	0.78(07)	1.05(24)	1.12(26)	1.28	[19]
^{150}Nd	0.22	3.04	3.12	3.12	3.13	1.61(09)	1.83(26)	1.83(26)	1.83	[19]
^{148}Sm	0.12	3.07	3.07	3.07	3.17	0.43(12)	0.51(12)	0.51(12)	0.46	[20]
^{150}Sm	0.16	3.13	3.18	3.18	3.17	0.92(06)	0.97(17)	0.97(17)	1.12	[20]
^{152}Sm	0.24	2.99	2.97	2.97	2.99	2.26(09)	2.41(33)	2.41(33)	2.50	[20]
^{154}Sm	0.26	3.20	3.26	3.14	3.10	2.18(12)	2.44(38)	2.76(50)	3.34	[20]
^{154}Gd	0.25	–	2.91	3.00	3.04	2.60(50)	2.99(62)	2.60(50)	3.00	[21]
^{156}Gd	0.26	3.06	3.06	2.94	3.09	2.73(27)	2.73(56)	3.22(68)	3.44	[21]
^{158}Gd	0.26	3.14	3.10	3.04	3.09	3.39(17)	3.71(59)	3.99(65)	3.52	[21]
^{160}Gd	0.27	3.18	3.11	3.10	3.14	2.97(12)	3.26(51)	4.41(54)	4.02	[22]
^{160}Dy	0.26	2.87	2.87	2.87	3.08	2.42(18)	2.42(30)	2.42(30)	3.60	[7]
^{162}Dy	0.26	2.96	2.93	2.84	3.07	2.49(13)	2.85(22)	3.30(24)	3.69	[23]
^{164}Dy	0.26	3.14	2.97	3.00	3.07	3.18(15)	3.25(43)	5.53(45)	3.80	[23]
^{166}Er	0.26	2.96	2.99	2.79	3.06	2.67(19)	2.55(48)	3.12(58)	3.86	[24]
^{168}Er	0.26	3.21	3.24	3.21	3.06	2.82(42)	3.68(48)	3.85(50)	3.95	[24]
^{170}Er	0.26	3.22	3.22	3.22	3.05	2.63(16)	3.42(69)	2.63(39)	4.03	[24]
^{172}Yb	0.25	3.03	3.03	2.93	2.99	1.94(22)	1.83(49)	2.37(49)	3.72	[25]
^{174}Yb	0.25	3.15	3.15	2.96	2.98	2.70(31)	2.70(88)	3.33(1.21)	3.80	[25]
^{176}Yb	0.24	2.96	3.33	2.86	2.92	2.66(34)	2.56(97)	3.24(1.05)	3.46	[25]
^{176}Hf	0.23	–	3.28	3.22	3.27	–	3.11(27)	3.32(28)	3.15	[26]
^{178}Hf	0.22	3.11	3.21	3.21	3.27	2.04(07)	2.38(36)	2.38(33)	3.20	[27]
^{180}Hf	0.22	2.95	3.19	3.16	3.22	1.61(07)	2.04(28)	2.13(30)	2.84	[27]
^{182}W	0.20	3.10	3.25	3.10	3.13	1.65(10)	1.34(23)	1.65(28)	2.03	[28]
^{184}W	0.19	3.31	3.37	3.19	3.08	1.12(17)	1.04(33)	1.24(37)	1.68	[28]
^{186}W	0.18	3.20	3.19	3.19	3.03	0.82(12)	0.82(21)	0.82(21)	1.36	[28]
^{190}Os	0.15	2.90	2.87	2.83	2.98	–	0.85(11)	0.94(12)	1.39	[29]
^{192}Os	0.14	3.01	3.00	3.00	2.94	–	0.93(06)	0.93(06)	0.99	[29]
^{194}Pt	0.13	–	3.25	3.25	2.97	–	1.38(25)	1.31(23)	1.17	[30]
^{196}Pt	0.12	2.68	3.01	2.70	2.95	–	0.81(16)	0.69(13)	0.86	[31]

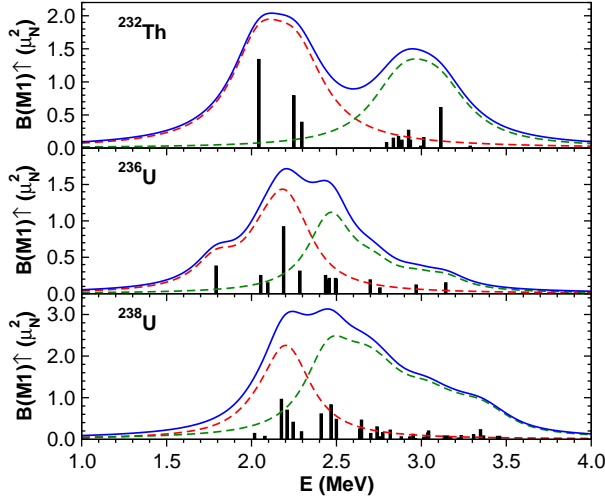


FIG. 5: The experimentally observed spectra of 1^+ excitations: ^{232}Th – [32], ^{236}U – [33], ^{238}U – [34].

the papers [15, 16]. Let us remind that in these papers the strengths of 1^+ excitations are summed in the energy interval $2.7 - 3.7$ MeV for $Z < 68$ and $2.4 - 3.7$ MeV for $Z \geq 68$. In Fig. 7(b,b') the theory results are compared with experimental data from the review [35], where the strengths of 1^+ excitations are summed in the energy interval $2.5 - 4$ MeV. It is seen, that here the agreement of the theory with experiment is a little bit better than on Fig. 7(a,a'). In Fig. 7(c,c') our theoretical results are compared with the sums of strengths of all 1^+ excitations observed in the energy interval $0 - 4$ MeV (let us call it variant " 1^+ "). Obviously, the agreement of the theory with experiment looks substantially better on Fig. 7(c,c') – the only exception is ^{164}Dy , which will be discussed later. The situation with ^{170}Er looks rather strange, because the energy interval used for Fig. 7(c,c') is wider than in the case of Fig. 7(b,b'). However, it seems that this problem is resolved in Fig. 7(d,d'), which demonstrates our theoretical results in comparison with the sums of strengths of all 1^+ excitations plus the sums of all 1^π excitations whose parity π is unknown (let us call it variant " 1^π "); the numerical information about this variant is contained in the second lines of Table II for the majority of nuclei). Really, the situations with ^{170}Er on Fig. 7(b,b') and Fig. 7(d,d') are very close to identical ones – probably the authors of [35] also took into account all 1^π excitations.

It is difficult to give a preference to variants " 1^+ " or " 1^π ". Both are equally good in the sense of the agreement of the theory with the experiment. After including 1^π levels the agreement obviously improved for 8 nuclei ($^{166,170}\text{Er}$, $^{172,174}\text{Yb}$, $^{178,180}\text{Hf}$, ^{186}W , ^{196}Pt) and it became worse for 9 other nuclei (^{134}Ba , $^{144,146}\text{Nd}$, ^{168}Er , ^{176}Yb , ^{176}Hf , $^{190,192}\text{Os}$, ^{194}Pt), the deterioration for 2 nuclei (^{168}Er , ^{194}Pt)

being rather small. In any case we choose the variant " 1^+ " as the basic one. The variant " 1^π " is useful in the sense of perspectives. One can expect that among 1^π excitations there are undoubtedly 1^+ states in the nuclei for which variant " 1^π " is better than variant " 1^+ ". On the other hand, in the nuclei where variant " 1^π " is worse than variant " 1^+ " one can expect that among 1^π excitations there are undoubtedly also 1^- states.

V. CRITERIA

So, the degree of agreement between our theory and an experiment strongly depends on the energy interval from which the 1^+ excitations are extracted and attributed to the scissors mode. What are the criteria for choosing the candidates belonging to a scissors mode? It may be useful to reproduce a rather long citation from Ref. [15] to answer this question:

"...those states around 3 MeV are considered to have positive parity that fulfill the condition $0 < R_{\text{Exp}} < 1$. This rule has exception as has been found in recent polarimeter measurements. In the nucleus ^{150}Nd , for instance, a rather strong 1^- state has been observed at an excitation energy of 2.414 MeV that shows a ground-state branching of $R_{\text{Exp}} < 1$ [36]. Moreover, a state with $R_{\text{Exp}} = 0.5$ at 3.751 MeV in the transitional nucleus ^{146}Nd has been identified to be a 1^- state [19]. Because of these exceptions it is useful to consider the excitation energy range as an additional signature for the fragments of the scissors mode. Therefore, only those states are assumed to contribute to the scissors mode where a decay to the 2_1^+ state has been observed with a branching ratio of $0 < R_{\text{Exp}} < 1$ and which lie within an energy range of $2.7 \text{ MeV} < E < 3.7 \text{ MeV}$ for $Z < 68$, and $2.4 \text{ MeV} < E < 3.7 \text{ MeV}$ for $Z \geq 68$ An additional argument to neglect ($\Delta K = 1$) strength below 2.7 MeV in the lighter rare earth nuclei is the existence of low-lying two-quasiparticle M1 excitations around 2.5 MeV as reported from a particle transfer experiment [37] on the nucleus ^{164}Dy ."

Later the authors of the paper [35] expanded the energy interval $2.7 - 3.7$ MeV to $2.5 - 4$ MeV preferring to announce about all exceptions from this "energy interval rule".

The lower bound 2.7 MeV was chosen in [15] to exclude the two-quasiproton excitation observed by authors of [37] in ^{164}Dy at the energy 2.557 ± 0.015 MeV. We are not sure that the observation of one "non-scissors" 1^+ level in one nucleus is a sufficient reason to exclude **all** 1^+ levels below 2.7 MeV in **all** nuclei. So, we prefer to take into account **all** 1^+ states below 4 MeV paying special attention to all possible exceptions.

One more citation, see Ref. [23]: "In ^{164}Dy ,

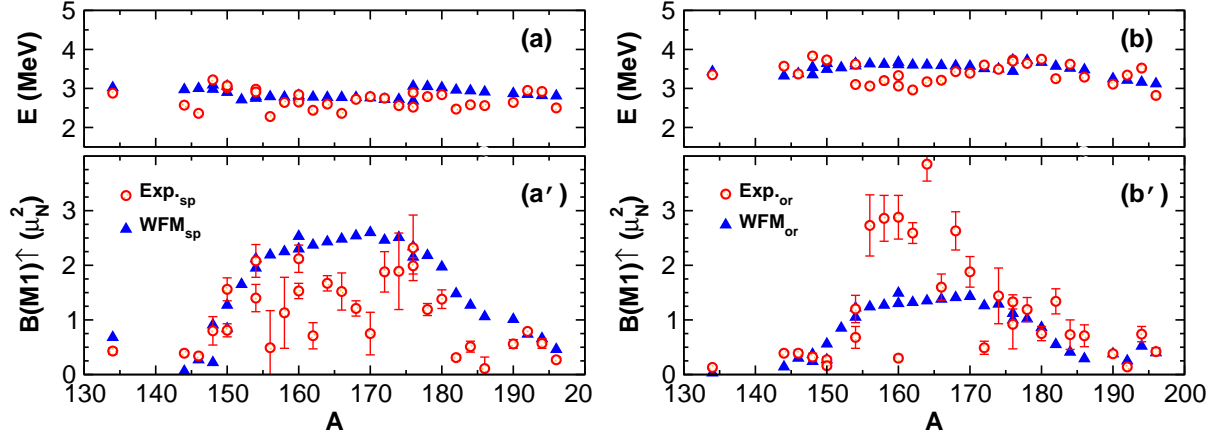


FIG. 6: Energies E and transition probabilities $B(M1)$ of the spin scissors and the orbital scissors obtained by dividing experimental spectra in two groups according to the rules of separation formulated in Sec. III; spectra are taken from papers shown in the last column of Table IV. WFM_{sp} and WFM_{or} – the results of calculation for spin and orbital scissors respectively; Exp_{sp} and Exp_{or} – experimental results for the same scissors.

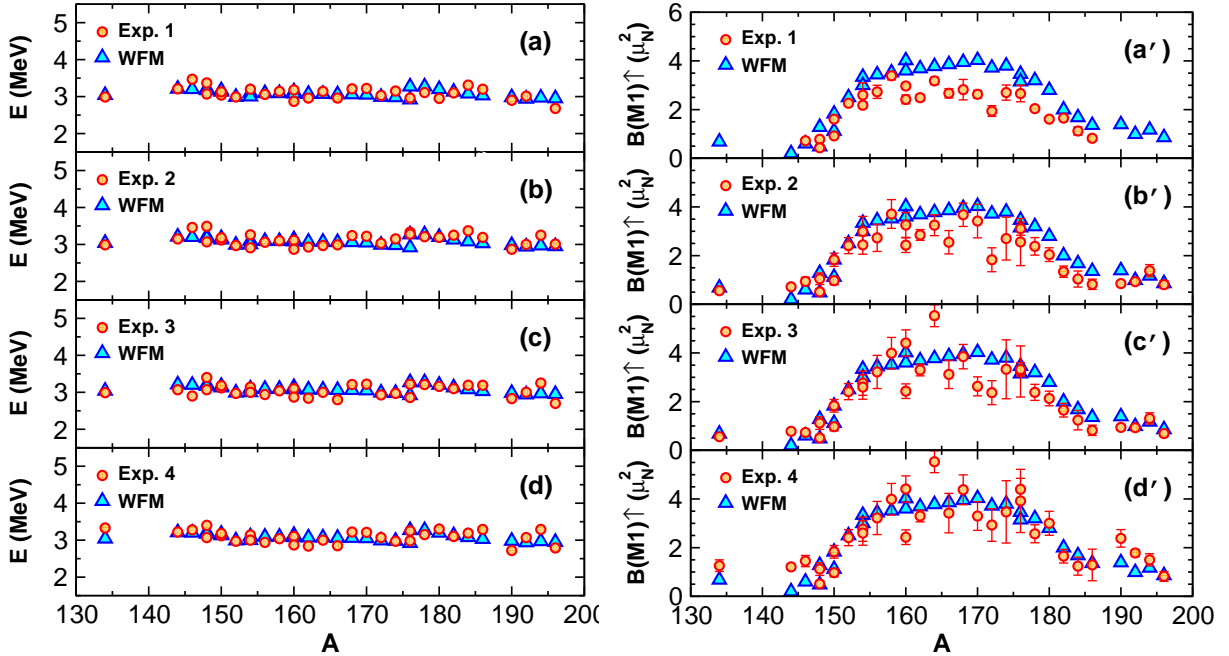


FIG. 7: Calculated (WFM) mean excitation energies (a,b,c,d) and summed $M1$ strengths (a',b',c',d') of the scissors mode are compared with different variants of experimental data treatment (see Sec. IV): (a,a'), Exp. 1 – experimental data from [15, 16] where only levels with $J^\pi = 1^+$ in the energy interval 2.7 – 3.7 MeV for $A < 164$ and 2.4 – 3.7 MeV for $A > 164$ are included; (b,b'), Exp. 2 – experimental data from [35] where only levels with $J^\pi = 1^+$ in the energy interval 2.5 – 4.0 MeV are included; (c,c'), Exp. 3 – the levels with $J^\pi = 1^+$ in the energy interval 0 – 4.0 MeV are included, experimental data are taken from papers shown in the last column of Table IV; (d,d'), Exp. 4 – the levels with $J = 1$ but π unknown (+ or - ?) are added to the levels of variant (c,c').

spin contributions have been found by Frekers and coworkers [38] around 3 MeV. Those are subtracted from the total strength assuming constructive interference.” One may conclude from here that one must not attribute to the scissors mode all levels excited by the spin dependent part of the external field (the spin part of the magnetic operator (11)). This statement looks quite natural when one studies the excitations of the orbital nature, to which the scissors mode belongs. However, our calculations do not confirm this. In fact, we compare the sum of calculated $B(M1)$ values of spin and orbital scissors with the sum of $B(M1)$ values of experimentally found **orbital** M1 excitations. One may see some contradiction in such a comparison. However all is correct. The point is that as a matter of fact **both our scissors have orbital nature**, because both are generated by the same type of collective variables – by the orbital angular momenta (the variables $L_{\lambda\mu}$ in (9) with $\lambda = \mu = 1$). All the difference is that the ”orbital” scissors are generated by the counter-oscillations of the orbital angular momentum of protons with respect of the orbital angular momentum of neutrons, whereas the ”spin” scissors are generated by the counter-oscillations of the orbital angular momentum of nucleons having the spin projection ”up” with respect of the orbital angular momentum of nucleons having the spin projection ”down”. **Both scissors are equally strongly sensitive to the influence of the spin part of the magnetic dipole operator (11).**

A. Sum rules for scissors mode

A very popular criterion for attributing observed 1^+ excitations to the scissors mode is the sum rule derived by LoIudice and Richter [39]:

$$B(M1) \uparrow \approx 0.0042 \frac{4NZ}{A^2} \omega_{sc} A^{5/3} (g_p - g_n)^2 \delta^2 [\mu_N^2].$$

Taking here $\omega_{sc} \simeq 3$ MeV, $g_n = 0$ and $g_p = 2Z/A$ one gets the following expression:

$$B(M1) \uparrow \approx 0.2016 N(Z/A)^3 A^{2/3} \delta^2 [\mu_N^2]. \quad (12)$$

The results given by this formula are shown on Fig. 8 by the multiplication signs. Later, the authors of [35] suggested a parameter free description of the scissors mode. Using the results of Lipparini and Stringari [40, 41] obtained with the help of the linearly and inverse energy-weighted sum rules, they derived the following two formulae (numbers (25) and (26) in [35]):

$$\sum B(M1) = \frac{3}{\pi} \sqrt{\frac{3}{20}} r_0 A^{5/6} \omega_D \sqrt{\frac{4NZ}{A^2}} \hbar \sqrt{\frac{\xi m_N}{\omega_{E2}}} g_{IS}^2 \delta, \quad (13)$$

$$\sum B(M1) = \frac{3}{\pi} \sqrt{\frac{\Upsilon}{50}} r_0^2 A^{5/6} \omega_D \sqrt{\frac{4NZ}{A^2}} m_N \sqrt{\xi} g_{IS}^2 \delta^2, \quad (14)$$

where $\xi = \omega_Q^2 / (\omega_Q^2 + 2\omega_D^2)$, ω_D and ω_Q are energy centroids of IsoVector Giant Dipole Resonance (IVGDR) and IsoScalar Giant Quadrupole Resonance (ISGQR) respectively, ω_{E2} is the excitation energy of the 2_1^+ state and g_{IS} is the gyromagnetic ratio of the ground-state (isoscalar) rotational band. ω_D and ω_Q are approximated by analytic expressions given in [42] and [43]. Inserting in (13) $r_0 = 1.2$ fm and experimental values of ω_{E2} from [44] and g_{IS} from [45] one gets the results marked on Fig. 8(a) as ”Sum Rule 1”.

Formula (14) is obtained from (13) by replacing ω_{E2} by some analytic expression [35] with the only parameter Υ . ”The average of Υ in the mass region considered here is 7.9 with typical deviations of about 10% (standard deviation).” The results of calculations by this formula with the same values of g_{IS} practically coincide with the ones given by formula (13). The remarkable feature of the calculated results is their extremely irregular, ”chaotic” distribution, that is connected undoubtedly with the microscopic (shell model) structure of each individual nucleus. For the sake of comparison with the WFM method and with the sum rule of LoIudice and Richter it would be more natural to use for g_{IS} in formula (14) some analytic expression common for all nuclei instead of experimental values. For example, a very well known expression is $g_{IS} = Z/A$. Another quite natural possibility is to take the average value \bar{g}_{IS} . The averaging over the considered group of nuclei gives $\bar{g}_{IS} = 0.33$. The results of calculations with both variants are shown in Fig. 8(b): Sum Rule 2 for $g_{IS} = Z/A$ and Sum Rule 2a for $g_{IS} = \bar{g}_{IS}$. The situation looks rather interesting. Obviously, one can find an ”optimal” value of g_{IS} for which the results will be settled in between the values of Sum Rule 2 and Sum Rule 2a. These values are compared with the results of WFM calculations in Fig. 8(c). As it is seen, the agreement is very good. Therefore one can conclude, that the results of the calculations with the WFM method and formula (14) (with proper choice of g_{IS}) are equally good to be used as the criteria for attributing observed 1^+ excitations to the scissors mode. One may wonder about this agreement and its underlying reason. Probably the spin dynamics, taken into account with the WFM method, is implicitly included by the experimental input data in expression (14).

VI. EXCEPTIONS

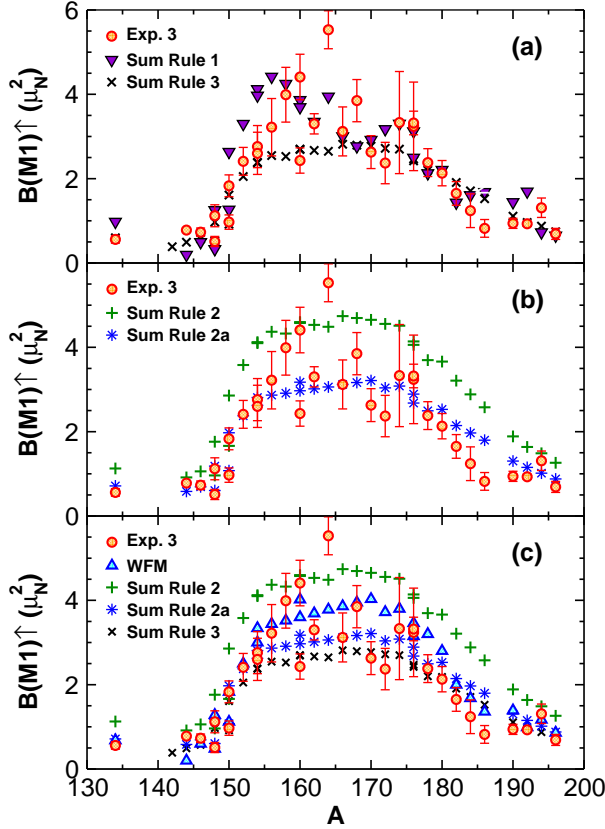


FIG. 8: The sum rule of LoIudice and Richter [39] (Sum Rule 3), the results given by formula (13) with experimental values of ω_{E2} and g_{IS} (Sum Rule 1), the results given by formula (14) with $g_{IS} = Z/A$ (Sum Rule 2) and $g_{IS} = \bar{g}_{IS}$ (Sum Rule 2a), and calculated (WFM) summed $M1$ strengths of the scissors mode are compared with experimental data (Exp. 3, variant (c') of Fig. 7).

The picture (c') of Fig. 7 demonstrates the strong deviation of the summed $B(M1)$ value of ^{164}Dy from the systematics of experimental data in the rare earths nuclei and from the theoretical result, whereas the picture (b') demonstrates their excellent agreement. This discrepancy was already explained in the section "Criteria". First reason is that we do not neglect by the levels excited by the spin dependent part of an external field. Second reason is connected with pure two-quasiparticle excitations. The authors of [37] say that the two-quasiproton excitation observed by them in ^{164}Dy at the energy 2.557 ± 0.015 MeV "probably corresponds either to the 1^+ state observed in (γ, γ') at 2.539 MeV or to that at 2.578 MeV with $B(M1) = 0.30 \mu_N^2$, and $0.46 \mu_N^2$, respectively." The structure of "the remaining 1^+ states near 2.5 MeV may involve quasiproton configurations associated with large $M1$ strength, but not accessible in the (t, α) reaction ..., or a **collective $M1$ interpretation may be appropriate.**" Our inference from this statement is that one

is free to interpret the remaining 1^+ states near 2.5 MeV as the members of the scissors mode – at least it is not forbidden by the experimental data. The exclusion of the pure two-quasiproton level (for example that one with $B(M1) = 0.46 \mu_N^2$) decreases the summed $B(M1)$ from $5.53 \mu_N^2$ to $5.07 \mu_N^2$, that as before strongly exceeds the result of calculation (see Table II) and does not fit the rare earths systematic. However, if to assume (following to [15, 23, 35]), that all levels near $E = 2.5$ MeV ($E = 2.531, 2.539, 2.578, 2.694$ MeV) have nearly pure two-quasiparticle nature, and not to take them into account, then one obtains $B(M1) = 3.85 \mu_N^2$ in excellent agreement with WFM result and with the rare earths systematic (see Tables I, II, IV). It is clear that the additional experimental and theoretical investigations are required to establish what kind of phenomenon is hidden behind of this group of levels. We hope that fourth order moments will be helpful in the resolution of this puzzle. Undoubtedly, RPA calculations could also be very useful.

^{192}Os

Following the indication of the Lorentzian curve one must put the border between the two parts of the spectrum at $E \simeq 3.35$ MeV, that leads to the following $M1$ strengths of the spin and orbital scissors: $B(M1)_{\text{sp}} = 0.86 \mu_N^2$ and $B(M1)_{\text{or}} = 0.07 \mu_N^2$. However, looking at Fig. 4 one easily finds another variant of the spectrum division – somewhere about $E = 3.15$ MeV. This variant of the border looks more attractive because in this case the distance between the respective levels $\Delta E = 193.5$ keV is bigger than in the variant dictated by the Lorentzian curve $\Delta E = 189$ keV. In this case the $M1$ strengths of the spin and orbital scissors become $B(M1)_{\text{sp}} = 0.79 \mu_N^2$ and $B(M1)_{\text{or}} = 0.14 \mu_N^2$ respectively, that is quite close to the theoretical values. Namely this variant is exhibited in the Table II and at Fig. 4.

^{154}Sm

The Lorentzian curve indicates here the border at $E \approx 2.7$ MeV leading to $B(M1)_{\text{sp}} = 0.33 \mu_N^2$ and $B(M1)_{\text{or}} = 2.43 \mu_N^2$ which are in an absolute disagreement with theoretical predictions. A more reasonable place for the border is seen very well without any Lorentzians (see Fig. 4): $E \approx 3.3$ MeV. Such a division of the spectrum gives $B(M1)_{\text{sp}} = 2.08 \mu_N^2$ and $B(M1)_{\text{or}} = 0.68 \mu_N^2$ values, which are substantially closer to the theoretical results, see Table II. Dashed curves at Fig. 4 correspond to this variant of the border.

^{238}U

Table III shows an unexpected large value of the summed $B(M1)$ in comparison with that of ^{236}U and ^{232}Th and with the theoretical result. The possible reason of this discrepancy was indicated by the authors of [34]: " $M1$ excitations are observed at approximately $2.0 \text{ MeV} < E_\gamma < 3.5 \text{ MeV}$ with a strong concentration of $M1$ states around 2.5 MeV. ... The

observed $M1$ strength may include states from both the scissors mode and the spin-flip mode, which are indistinguishable from each other based exclusively on the use of the NRF technique.”

The most reasonable (and quite natural) place for the border between the scissors mode and the spin-flip resonance is located in the spectrum gap between 2.5 MeV and 2.63 MeV. The summed $M1$ strength of scissors in this case becomes $B(M1) = 4.38 \pm 0.5 \mu_N^2$ in rather good agreement with ^{236}U and ^{232}Th . This value is also not so far from the theoretical result. After dividing in spin and orbital scissors it gives $B(M1)_{\text{or}} = 1.92 \mu_N^2$ in good agreement with the calculated value.

Another candidate for the border between the scissors mode and the spin-flip resonance is the small gap disposed at $E \approx 2.85$ MeV. In this case the summed $M1$ strength of scissors is $B(M1) = 5.97 \pm 0.8 \mu_N^2$ in complete disagreement with the ^{236}U and ^{232}Th nuclei. Nevertheless this value is again not so far from the theoretical result. After dividing in spin and orbital scissors it gives $B(M1)_{\text{or}} = 3.51 \mu_N^2$ what is too far from the calculated value.

So, the first variant of a border is more preferable.

VII. CONCLUSIONS AND OUTLOOK

The aim of this paper was to find experimental indications about the existence of the ”spin” scissors mode predicted in our previous publications [1, 4, 5]. To this end we have performed the detailed analysis of experimental data on 1^+ excitations for nuclei of $N = 82 - 126$ major shell and for actinides.

We have found good quantitative agreement between the theory and experiment for the summed $B(M1)$ values and the respective energy centroids for the majority of nuclei except for some few, especially ^{164}Dy . The best agreement is obtained when one attributes to the scissors mode all 1^+ excitations observed in the energy interval $0 < E < 4$ MeV (excluding separate levels in some nuclei). It turns out also that the results of our calculations are in

very good agreement (see Fig. 8) with the sum rule derived in [35].

For the fine structure of the scissors mode in rare earth nuclei satisfactory (mostly very good) agreement between the theory and experiment is observed in 13 nuclei (see section ”Splitting”); in the rest of nuclei the situation is indefinite and requires further theoretical (and maybe experimental) study. In actinides very good agreement is observed for ^{232}Th , satisfactory agreement in ^{236}U , and a rather conditional one in ^{238}U .

It is shown that both scissors are strongly influenced by the spin dependent part of nuclear forces, so the observed 1^+ states having a spin nature may also be attributed to the scissors mode.

To gain the comprehensive insight into the fine structure of the scissors mode we are going to perform the calculations with fourth order moments which, as we hope, will allow us to expand substantially the set of input data for the WFM method and to study the dynamics of the spin-flip resonance and its possible influence on the scissors mode. Furthermore the self consistent RPA calculations with realistic forces are very desirable because they can give the information on the microscopic structure of 1^+ states, which is required to confirm the pure two-quasiparticle nature of some experimental levels.

A final observation: the modern experimental information is enough to conclude that the existence of spin (together with spin-orbital interaction) leads to the splitting of the scissors mode into two branches corresponding to spin and orbital scissors.

Acknowledgments

We wish to thank M. Guttormsen and J. N. Wilson for fruitful discussions, and P. von Neuman-Cosel who attracted our attention to the paper of A. S. Adekola et al [32]. The work was supported by the IN2P3/CNRS-JINR Collaboration agreement.

-
- [1] E. B. Balbutsev, I.V. Molodtsova, and P. Schuck, Nucl. Phys. A **872**, 42 (2011).
 - [2] N. Lo Iudice, La Rivista del Nuovo Cimento **23**(9), 1 (2000).
 - [3] K. Heyde, P. von Neuman-Cosel, and A. Richter, Rev. Mod. Phys. **82**, 2365 (2010).
 - [4] E. B. Balbutsev, I.V. Molodtsova, and P. Schuck, Phys. Rev. C **88**, 014306 (2013).
 - [5] E. B. Balbutsev, I.V. Molodtsova, and P. Schuck, Phys. Rev. C **91**, 064312 (2015).
 - [6] M. Guttormsen, L. A. Bernstein, A. Bürger, A. Gørgen, F. Gunsing, T.W. Hagen, A. C. Larsen, T. Renstrøm, S. Siem, M. Wiedeking, and J. N. Wilson, Phys. Rev. Lett. **109**, 162503 (2012).
 - [7] C. Wesselborg, P. von Brentano, K. O. Zell, R. D. Heil, H. H. Pitz, U. E. P. Berg, U. Kneissl, S. Lindenstruth, U. Seemann, and R. Stock, Phys. Lett. B **207**, 22 (1988).
 - [8] P. Ring and P. Schuck, *The Nuclear Many-Body Problem* (Springer, Berlin, 1980).
 - [9] E. B. Balbutsev and P. Schuck, Nucl. Phys. A **720**, 293 (2003); A **728**, 471 (2003).
 - [10] D. A. Varshalovitch, A. N. Moskalev, and V. K. Khersonski, *Quantum Theory of Angular Momen-*

- tum (World Scientific, Singapore, 1988).
- [11] E. B. Balbutsev and P. Schuck, Nucl. Phys. A **652**, 221 (1999).
 - [12] E. B. Balbutsev and P. Schuck, Ann. Phys. **322**, 489 (2007).
 - [13] E. B. Balbutsev, L. A. Malov, P. Schuck, M. Urban, and X. Viñas, Phys. At. Nucl. **71**, 1012 (2008).
 - [14] E. B. Balbutsev, L. A. Malov, P. Schuck, and M. Urban, Phys. At. Nucl. **72**, 1305 (2009).
 - [15] N. Pietralla, P. von Brentano, R.-D. Herzberg, U. Kneissl, J. Margraf, H. Maser, H. H. Pitz, and A. Zilges, Phys. Rev. C **52**, R2317 (1995).
 - [16] N. Pietralla, P. von Brentano, R.-D. Herzberg, U. Kneissl, N. Lo Iudice, H. Maser, H. H. Pitz, and A. Zilges, Phys. Rev. C **58**, 184 (1998).
 - [17] H. Maser, N. Pietralla, P. von Brentano, R.-D. Herzberg, U. Kneissl, J. Margraf, H. H. Pitz, and A. Zilges, Phys. Rev. C **54**, R2129 (1996).
 - [18] T. Eckert, O. Beck, J. Besserer, P. von Brentano, R. Fischer, R.-D. Herzberg, U. Kneissl, J. Margraf, H. Maser, A. Nord, N. Pietralla, H. H. Pitz, S. W. Yates, and A. Zilges, Phys. Rev. C **56**, 1256 (1997).
 - [19] J. Margraf, R. D. Heil, U. Kneissl, U. Maier, H. H. Pitz, H. Friedrichs, S. Lindenstruth, B. Schlitt, C. Wesselborg, P. von Brentano, R.-D. Herzberg, and A. Zilges, Phys. Rev. C **47**, 1474 (1993).
 - [20] W. Ziegler, N. Huxel, P. von Neumann-Cosel, C. Rangacharyulu, A. Richter, C. Spieler, C. de Coster, and K. Heyde, Nucl. Phys. A **564**, 366 (1993).
 - [21] H. H. Pitz, U. E. P. Berg, R. D. Heil, U. Kneissl, R. Stock, C. Wesselborg, and P. von Brentano, Nucl. Phys. A **492**, 411 (1989).
 - [22] H. Friedrichs, D. Häger, P. von Brentano, R. D. Heil, R.-D. Herzberg, U. Kneissl, J. Margraf, D. Müller, H. H. Pitz, B. Schlitt, M. Schumacher, C. Wesselborg, and A. Zilges, Nucl. Phys. A **567**, 266 (1994).
 - [23] J. Margraf, T. Eckert, M. Rittner, I. Bauske, O. Beck, U. Kneissl, H. Maser, H. H. Pitz, A. Schiller, P. von Brentano, R. Fischer, R.-D. Herzberg, N. Pietralla, A. Zilges, and H. Friedrichs, Phys. Rev. C **52**, 2429 (1995).
 - [24] H. Maser, S. Lindenstruth, I. Bauske, O. Beck, P. von Brentano, T. Eckert, H. Friedrichs, R. D. Heil, R.-D. Herzberg, A. Jung, U. Kneissl, J. Margraf, N. Pietralla, H. H. Pitz, C. Wesselborg, and A. Zilges, Phys. Rev. C **53**, 2749 (1996).
 - [25] A. Zilges, P. von Brentano, C. Wesselborg, R. D. Heil, U. Kneissl, S. Lindenstruth, H. H. Pitz, U. Seemann, and R. Stock, Nucl. Phys. A **507**, 399 (1990).
 - [26] M. Scheck, D. Belic, P. von Brentano, J. J. Carroll, C. Fransen, A. Gade, H. von Garrel, U. Kneissl, C. Kohstall, A. Linnemann, N. Pietralla, H. H. Pitz, F. Stedile, R. Toman, and V. Werner, Phys. Rev. C **67**, 064313 (2003).
 - [27] N. Pietralla, O. Beck, J. Besserer, P. von Brentano, T. Eckert, R. Fischer, C. Fransen, R.-D. Herzberg, D. Jäger, R. V. Jolos, U. Kneissl, B. Krischok, J. Margraf, H. Maser, A. Nord, H. H. Pitz, M. Rittner, A. Schiller, and A. Zilges, Nucl. Phys. A **618**, 141 (1997).
 - [28] R.-D. Herzberg, A. Zilges, P. von Brentano, R. D. Heil, U. Kneissl, J. Margraf, H. H. Pitz, H. Friedrichs, S. Lindenstruth, and C. Wesselborg, Nucl. Phys. A **563**, 445 (1993).
 - [29] C. Fransen, B. Krischok, O. Beck, J. Besserer, P. von Brentano, T. Eckert, R.-D. Herzberg, U. Kneissl, J. Margraf, H. Maser, A. Nord, N. Pietralla, H. H. Pitz, and A. Zilges, Phys. Rev. C **59**, 2264 (1999).
 - [30] A. Linnemann, P. von Brentano, J. Eberth, J. Enders, A. Fitzler, C. Fransen, E. Guliyev, R.-D. Herzberg, L. Käubler, A. A. Kuliev, P. von Neumann-Cosel, N. Pietralla, H. Prade, A. Richter, R. Schwengner, H. G. Thomas, D. Weisshaar, and I. Wiedenhöver, Phys. Lett. B **554**, 15 (2003).
 - [31] P. von Brentano, J. Eberth, J. Enders, L. Esser, R.-D. Herzberg, N. Huxel, H. Meise, P. von Neumann-Cosel, N. Nicolay, N. Pietralla, H. Prade, J. Reif, A. Richter, C. Schlegel, R. Schwengner, S. Skoda, H. G. Thomas, I. Wiedenhöver, G. Winter, and A. Zilges, Phys. Rev. Lett. **76**, 2029 (1996).
 - [32] A. S. Adekola, C. T. Angell, S. L. Hammond, A. Hill, C. R. Howell, H. J. Karwowski, J. H. Kelley, and E. Kwan, Phys. Rev. C **83**, 034615 (2011).
 - [33] J. Margraf, A. Degener, H. Friedrichs, R. D. Heil, A. Jung, U. Kneissl, S. Lindenstruth, H. H. Pitz, H. Schacht, U. Seemann, R. Stock, C. Wesselborg, P. von Brentano, and A. Zilges, Phys. Rev. C **42**, 771 (1990).
 - [34] S. L. Hammond, A. S. Adekola, C. T. Angell, H. J. Karwowski, E. Kwan, G. Rusev, A.P. Tonchev, W. Tornow, C. R. Howell, and J. H. Kelley, Phys. Rev. C **85**, 044302 (2012).
 - [35] J. Enders, P. von Neumann-Cosel, C. Rangacharyulu, and A. Richter, Phys. Rev. C **71**, 014306 (2005).
 - [36] H. Friedrichs, B. Schlitt, J. Margraf, S. Lindenstruth, C. Wesselborg, R. D. Heil, H. H. Pitz, U. Kneissl, P. von Brentano, R.-D. Herzberg, A. Zilges, D. Häger, G. Müller, and M. Schumacher, Phys. Rev. C **45**, R892 (1992).
 - [37] S. J. Freeman, R. Chapman, J. L. Durell, M. A. C. Hotchkis, F. Khazaie, J. C. Lisle, J. N. Mo, A. M. Bruce, R. A. Cunningham, P. V. Drumm, D. D. Warner, and J. D. Garrett, Phys. Lett. B **222**, 347 (1989).
 - [38] D. Frekers, H.J. Wörtche, A. Richter, R. Abegg, R. E. Azuma, A. Celler, C. Chan, T.E. Drake, R. Helmer, K.P. Jackson, J.D. King, C.A. Miller, R. Schubank, M. C. Vetterli, and S. Yen, Phys. Lett. B **244**, 178 (1990).
 - [39] N. LoIudice and A. Richter, Phys. Lett. B **304**, 193 (1993).
 - [40] E. Lipparini and S. Stringari, Phys. Lett. B **130**, 139 (1983).
 - [41] E. Lipparini and S. Stringari, Phys. Rep. **175**, 103 (1989).
 - [42] B.L. Berman and S.C. Fultz, Rev. Mod. Phys. **47**, 713 (1975).
 - [43] A. van der Woude, in *Electric and Magnetic Giant Resonances in Nuclei*, edited by J. Speth (World Scientific, Singapore, 1991), p. 99.
 - [44] S. Raman, C.H. Malarkey, W.T. Milner, C.W. Nestor, Jr., and P.H. Stelson, At. Data Nucl. Data Tables **36**, 1 (1987).

- [45] N. J. Stone, At. Data Nucl. Data Tables **90**, 75 (2005).